Reports

Radiative Properties of the Background Aerosol: Absorption Component of Extinction

Abstract. *The light-scattering and light-absorption coefficients of the global background aerosol define its single-scatter albedo. Continuous, simultaneous measurements of these optical coefficients were made on a daily basis for the remote marine mid-troposphere; such measurements are essential for assessment of the effects of aerosol on atmospheric radiative transfer. Measurements of light-absorption coefficients made at the Mauna Loa Observatory in Hawaii were higher than expected, and the single-scatter albedo was lower than the value often used in radiative transfer models. Soot appears to be the most likely primary absorber, and hemispheric dispersal of this combustion-derived material is suggested.*

Antony D. Clarke
Robert J. Charlson
Environmental Engineering and Sciences Program, University of Washington, Seattle 98195

Atmospheric radiative transfer (*1*, *2*) and hence climate can be affected by various kinds of aerosol, including volcanic emissions (*3*), pollutants transported to the Arctic (*4*) and those dispersed to remote areas (*5*), outbreaks of desert dust from Asia or the Sahara (*6*), and smoke generated after a nuclear war (*7*). Measurements of the light-absorption coefficient b_a, and of the single-scatter albedo, $\tilde{\omega}$, have been reported for polluted continental regions or during intrusions of polluted air to remote areas. However, the low values of b_a in the remote background troposphere have prevented its measurement for sampling times shorter than synoptic meteorological events. The integrating sandwich (*8*), which is useful for measuring values of b_a as low as 10^{-8} m^{-1} within an 8-hour period, has removed this limitation.

The Mauna Loa Observatory, located at an altitude of 3400 m, approximately 1500 m above the marine trade wind inversion, is an ideal site for measuring the remote background troposphere. We assume that the samples we describe here are representative of the Pacific background aerosol. A local upslope-downslope surface circulation is superimposed on the synoptic wind pattern (*9*). During upslope flow (day), polluted air below the inversion layer can be carried up the slopes to the observatory. Consequently, data for 1982 were collected between 22:00 and 7:00 (local standard time) during downslope flow (night) (*10*) and for modified Julian days (JD) 115 to 152 (25 April to 1 June; period A) and JD 197 to 345 (16 July to 11 December; period B) (In this modification of the Julian calendar, days are numbered from 1 January of each year.) Data for 1983 are not included because of frequent perturbations from local volcanic activity. These two sampling periods represent active and inactive transport of Asian dust to the observatory. In a concurrent study (*11*), downslope mean concentrations of crustal dust of about 600 and 64 ng m^{-3} were recorded for the same two periods, respectively. Corresponding measurements of sulfate, the other major component of the aerosol, were approximately 480 and 240 ng m^{-3}.

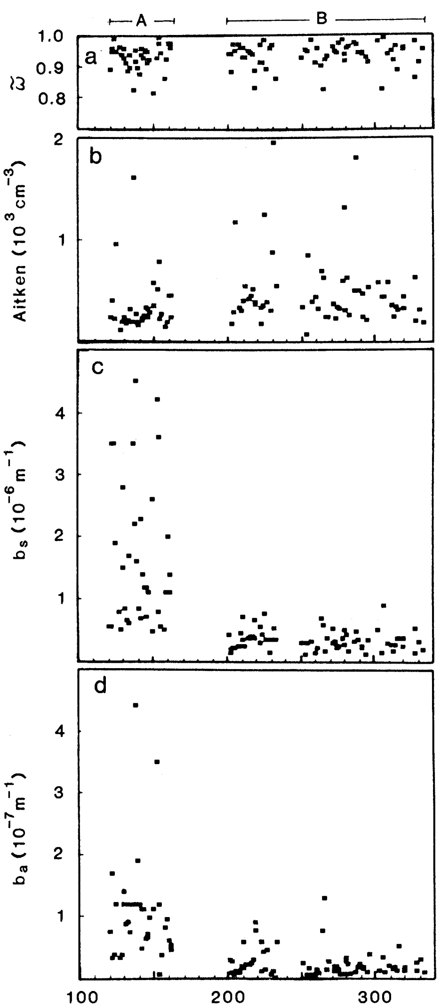

Fig. 1. Time series of nightly downslope aerosol data from Mauna Loa Observatory, 1982. (a) Single-scatter albedo. (b) Condensation nuclei count. (c) Light-scattering coefficient, b_s (550 nm). (d) Light-absorption coefficient, b_a (550 nm). Apparent data coincidence is due to plot resolution.

Aerosol samples were collected nightly on quartz fiber filters (Pallflex QAS 2500, 25 mm in diameter) at flow rates of 60 liters per minute. Some filters were not changed on weekends; these samples represent collections for three consecutive nights and were averaged over that time. Two filters, one with and one without a modified cyclone (Bendix model 18) were used simultaneously to obtain size segregation. The cyclone operated with a 50 percent cutoff for particles about 0.7 μm in diameter (density, 1.5 g cm^{-3}) so that coarse particles could be removed. An optical particle counter (Royco model 220) was used to obtain size distributions (0.3 to 8.0 μm) during period A. A bimodal distribution was observed with an intermode mass minimum at a particle diameter of about 0.5 μm. The fine-mode aerosol had a mass peak near 0.3 μm, and the peak for the coarse-mode mass was near 3 μm. Little coarse mass was observed below 1 μm, which justified the choice of the cyclone's size cutoff. Measurements of b_a from both filters made it possible to calculate the contribution to b_a from the coarse and fine modes by difference. An integrating nephelometer (*12*) provided 1-minute means of the light-scattering coefficient, b_s, that were later averaged over the 8-hour sampling periods for comparison to b_a and for evaluation of $[\tilde{\omega} = b_s/(b_s + b_a)]$. Counts for condensation nuclei (CN) were similarly averaged and used as an index of the presence of contaminated air at the observatory.

Figure 1 is a time series of data from 1982 for b_a, b_s, CN counts, and $\tilde{\omega}$ for both sampling periods. Systematic error in b_s was possible because of angular truncation in the nephelometer and may have approached 10 percent (at 550 nm). Random error in b_s decreased with averaging time and was much less than 10 percent for these 8-hour periods. Systematic error due to absorption calibration was about 20 percent for b_a (*8*), which could yield a 1.3 percent uncertainty in $\tilde{\omega}$ at the average value of 0.93.

Table 1. Averaged aerosol data from the Mauna Loa Observatory obtained in 1982. Numbers in parentheses are the number of samples obtained during periods A and B. Values are reported ±1 standard deviation.

Julian day	b_s ($m^{-1} \times 10^{-7}$)	b_a ($m^{-1} \times 10^{-8}$)	Condensation nuclei (number of particles per cubic centimeter)	$\tilde{\omega}$	$1 - R$ (percent of b_a in coarse mode)	Estimated percent of b_a due to dust*
115 to 152	16.1 ± 11.6 (35)	12.3 ± 13.9 (35)	341 ± 285 (33)	0.926 ± 0.041 (33)	0.27	0.35
197 to 345	3.53 ± 1.67 (66)	2.45 ± 2.25 (66)	498 ± 426 (64)	0.935 ± 0.039 (64)	0.22	0.18
115 to 345	8.08 ± 9.27 (112)	5.86 ± 9.95 (101)	446 ± 387 (98)	0.931 ± 0.041 (101)	0.24	0.24

*Estimated from concentrations of aerosol dust (*12*) and an estimated specific absorption for Asian dust of 0.07 $m^2 g^{-1}$.

Random errors in b_a due to uncertainties in measurement and flow were typically less than 10 percent as judged from many simultaneous measurements made earlier. Period A had numerous values for b_a and b_s that exceeded period B by a factor of 5 or more. However, CN counts were generally higher during period B and only rarely coincided with the higher b_a values. Because combustion results in elevated CN counts in conjunction with higher values for b_a, local combustion sources are not implicated from the variability of these data. Progressive changes in aerosol concentrations often occurred over several day-night periods and were consistent with synoptic scale variability in air masses subject to long distance transport.

The mean ratio, R, of values for b_a measured on the "cycloned" filter (fine mass fraction) to those for b_a measured on the "total" filter was 0.73 for period A and 0.78 for period B (Table 1). Hence, only 27 percent ($1 - R$) of the absorption during period A and 22 percent during period B appears to be related to coarse particles. In several samples analyzed by scanning electron microscopy (SEM), the coarse-mode particles were identified as primarily crustal, whereas fine particles had properties resembling those of sulfate aerosol and had much higher sulfur concentrations, as determined by SEM energy-dispersive x-ray analysis. Three random, paired filter samples (period A) analyzed by ion chromatography (IC) gave ratios of cycloned fine-mass sulfate to total sulfate of 0.80, 0.78, and 0.80 (±12 percent, uncertainty in IC measurements). Hence, the fine mode mass is essentially noncrustal but accounts for most of the aerosol light absorption and sulfate mass.

The specific absorption, B_m, of Asian dust is unknown, but common values for crustal dust are between 0.02 and 0.1 $m^2 g^{-1}$ at 550 nm. When a value for B_m of 0.07 $m^2 g^{-1}$ (*13*) is used [obtained by the integrating sandwich technique for a standard crustal test dust (Arizona road dust, AZRD), the dust concentrations mentioned above imply mean values of b_a (equal to B_m times mass concentration) due to dust of 0.42×10^{-7} and 0.045×10^{-7} m^{-1} for periods A and B, respectively. These are four times lower than the means measured at the observatory for these periods. However, they are in reasonable agreement with the fraction ($1 - R$) of measured b_a that we attribute to the coarse-mode crustal aerosol for each period (Table 1) as judged by the size-segregated absorption measurements. Typical values of $\tilde{\omega}$ for crustal dusts are about 0.97 to 0.99 (AZRD, 0.98), although very low values of $\tilde{\omega}$ (0.86) have been measured for the highly absorbing red Saharan dust (*6*). Hence, a typical mixed crustal-sulfate aerosol should have values of $\tilde{\omega}$ near 0.98. The mean value of $\tilde{\omega}$ was about 0.93 for both periods A and B in spite of large changes in b_a and b_s (Table 1). This implies that the mean absorption is approximately four times greater than expected for a crustal background aerosol, and at times it is much greater. More than 90 percent of the data for both periods A and B were well above the line corresponding to crustal components with an $\tilde{\omega}$ of 0.98 (Fig. 2). Under conditions of elevated dust and in the absence of a stronger absorbing component, $\tilde{\omega}$ for Asian dust is defined by those data points (Fig. 2a) with the lowest value of $\tilde{\omega}$. Except for one low observation, these points define a line between C and D (Fig. 2a) corresponding to $\tilde{\omega}$ of 0.97. Most of the data are above such a line and indicate the presence of another fine particle component more absorbing than the dust.

The values reported for b_a and $\tilde{\omega}$ allow us to assess current radiative effects and may serve as a gauge for future trends. The data indicate that b_a is dominated by the fine-mode aerosol and is markedly higher than expected for dust alone, although it is elevated during the same periods when Asian dust and sulfates are transported to the observatory. Because no significant sources of oceanic light-

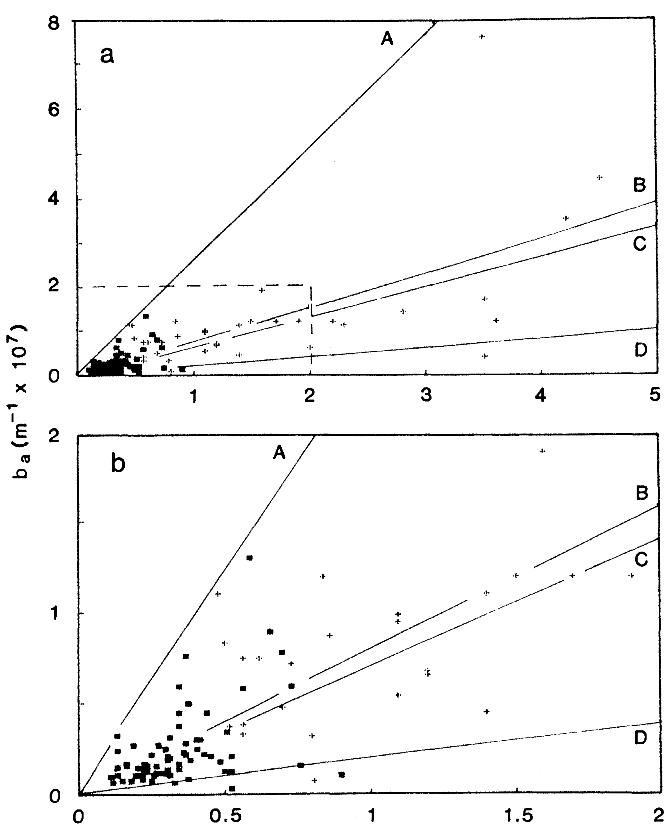

Fig. 2. Scatter plot of aerosol light-absorption coefficient, b_a, against scattering coefficient, b_s, for Mauna Loa Observatory data for Asian dust period (+) and normal period (■) in 1982. (a) Plot for all data. (b) Plot for rescaled data indicated by box in (a). Lines correspond to single-scatter albedo values for (A) rural average (0.8), (B) Asian dust (period A) average (0.925), (C) normal (period B) average (0.935), and (D) Arizona road dust reference value (0.98).

absorbing aerosol are known, and because local island sources are not evident, we suggest that most fine-particle absorption is, like Asian dust, transported from the continents and may be elemental carbon of submicrometer size that originated from combustion (soot). If the specific absorption of soot (~8.5 $m^2 g^{-1}$) is used to convert mean b_a values for the fine mode to soot concentrations, we obtain 12 ng m^{-3} for period A and 2.5 ng m^{-3} for period B; these values are not unlike minima reported for the remote Atlantic (20 ng m^{-3}) (*14*). Although soot concentrations are too low to be analyzed chemically on these filters, samples with more concentrated quantities or analyzed by spectral absorption (or both) may be useful in verifying our suggestion. If it is true, it implies that dispersal of combustion-derived aerosol may persist throughout the troposphere and over hemispheric spatial scales.

References and Notes

1. T. P. Ackerman and O. B. Toon, *Appl. Opt.* **20**, 3661 (1981).
2. J. M. Mitchell, *J. Appl. Meteorol.* **10**, 703 (1971).
3. O. B. Toon and J. B. Pollack, *ibid.* **15**, 225 (1976).
4. A. D. Clarke, R. J. Charlson, L. F. Radke, *Geophys. Res. Lett.* **11**, 5 (1981).
5. R. J. Ball and G. D. Robinson, *J. Appl. Meteorol.* **21**, 171 (1982).
6. T. N. Carlson and R. S. Caverly, *J. Geophys. Res.* **82**, 3141 (1977).
7. S. L. Thompson, *Ambio* **13**, 236 (1984).
8. A. D. Clarke, *Appl. Opt.* **21**, 3011 (1982).
9. B. G. Mendonca and W. T. Iwaoka, *J. Appl. Meteorol.* **8**, 213 (1969).
10. This time-based removal of upslope contamination was recently shown to be good (*11*), although a new multivariable monitor-controller is claimed to perform about 25 percent better in eliminating contamination.
11. J. R. Parrington, W. H. Zoller, N. K. Aras, *Science* **220**, 195 (1983).
12. B. A. Bodhaine, *J. Geophys. Res.* **88**, 10753 (1983).
13. A. D. Clarke and A. P. Waggoner, *Appl. Opt.* **21**, 398 (1982).
14. M. O. Andreae, *Science* **220**, 1148 (1983).

15. We thank K. Coulson, T. Defoor, and the staff of the Mauna Loa Observatory for daily sample collection, and B. Bodhaine for aerosol data from the observatory. This research was supported in part by NOAA under grant NA 79RAD00018.

1 November 1984; accepted 11 March 1985

Invasion and Extinction in the West Indian Ant Fauna: Evidence from the Dominican Amber

Abstract. *Of 37 genera and well-defined subgenera identified in the amber of the Dominican Republic (late Oligocene or early Miocene), 34 have survived somewhere in the New World tropics to the present, although the species studied thus far are extinct. Of the surviving genera and subgenera, 22 persist on Hispaniola. Fifteen genera and subgenera have colonized the island since amber times, restoring the number of genera and well-defined subgenera now present on Hispaniola to 37. A higher extinction rate has occurred in genera and subgenera that are either highly specialized or possess less colonizing ability, as evidenced by their restriction to the New World.*

EDWARD O. WILSON
Museum of Comparative Zoology,
Harvard University,
Cambridge, Massachusetts 02138

The amber of the Dominican Republic, which contains large numbers of well-preserved insect remains, provides an unusual opportunity to study evolution and extinction in an insular fauna. The most abundant insects in the amber are the ants. Baroni Urbani and Saunders (*1, 2*) recorded the presence of the Neotropical genera *Anochetus, Gnamptogenys, Paracryptocerus, Pseudomyrmex,* and *Trachymyrmex*. Additional specimens placed by Baroni Urbani (*3*) in *Leptomyrmex*, which is today restricted to the Indo-Australian region, have recently been transferred to the Neotropical *Camponotus branneri* group (*4*). I have been able to study 602 pieces of amber containing an estimated 1254 ants; most of these pieces were accumulated during the past 10 years at the Museum of Comparative Zoology, Harvard University (*5*). The diversity at the generic and specific level parallels that found in the contemporary Hispaniolan fauna (*6*): 37 genera and well-marked subgenera are now known from the Dominican amber, and an identical number have been found on present-day Hispaniola. Twenty-two of the genera and subgenera in the two chronofaunas are the same (Table 1).

Although additional genera will undoubtedly be found in both the amber deposits and the living fauna, the lists in Table 1 can be regarded as including a large majority of the complete faunas for two reasons. First, the considerable collections of Baltic amber ants studied by Mayr (*7*) and Wheeler (*8*) (10,988 specimens) were found to represent 43 genera. Although this diverse Oligocene fauna is thus known from about ten times as many specimens, it contains only six more genera than the Dominican amber fauna, a difference of 16 percent. Second, collections of the modern faunas made in Haiti and the Dominican Republic have been reasonably thorough (*6*). Studies of other islands in the Greater Antilles, namely, Cuba (*9*), Jamaica (*10*), and Puerto Rico (*11*), have yielded lists consistent with a projection of the contemporary Hispaniolan fauna of not many more than 40 genera and well-marked subgenera.

The exact age of the Dominican amber has not yet been determined, but combined stratigraphic and foraminiferal analyses of its matrix suggest that most of the deposits originated no later than the early Miocene (*2*). I favor the minimal age (about 20 million years) or at most a late Oligocene origin. Only three of the 37 Dominican amber genera, or 8 percent, are unknown from the contemporary world fauna and hence can be provisionally considered extinct (Table 1). This condition contrasts with that of the Baltic amber, which is Eocene to early Oligocene in age (*12*) and of which 44 percent are extinct genera; that is, 19 of the 43 genera recorded to date are unknown among living ants (*8*). The Dominican amber ants also differ to a similar degree from the 20 genera of the shales from Florissant, Colorado, which are upper Oligocene in age and include eight, or 40 percent, that are now evidently extinct (*13*).

Most of the pieces of Dominican amber came from the western amber-bearing region, located in the mountainous La Cumbre region 10 to 20 km northeast of Santiago. A few came from the eastern amber-bearing region south of Sabana de la Mar. Still others originated from Cotui, more centrally located. The Cotui pieces, making up fewer than 5 percent of the specimens I have seen, are evidently much younger than those from other Dominican localities (*14*); for that reason I excluded them from the present analysis. The most common ant species, *Azteca alpha*, occurs in pieces from nearly all the localities, as well as in the same pieces as seven of the genera other than *Azteca*.

To provide a first analysis of the history of the Dominican fauna, I classified the amber and living genera into six biogeographic categories (Table 1). The traits considered were the presence or absence of the genera in the amber and the extent of their retreat since amber times. The lists from the modern fauna were based on regional monographs of all of the islands of the Greater Antilles (*6, 9–11, 15*), together with more recent collections made in Cuba, the Dominican Republic, and Puerto Rico by W. L. Brown and me. In addition to the generic identifications of the amber fauna, I have